Compressive Echelle Spectroscopy

Lina Xu[a], Mark A. Davenport[b], Matthew A. Turner[a], Ting Sun[a], Kevin F. Kelly[a]
[a]Dept. of Electrical and Computer Engineering, Rice University, 6100 Main St., Houton, TX, 77005
[b]Dept. of Statistics, Stanford University, 390 Serra Mall, Sequoia Hall, Stanford, CA 94305

ABSTRACT

Building on the mathematical breakthroughs of compressive sensing (CS), we developed a 2D spectrometer system that incorporates a spatial light modulator and a single detector. For some wavelengths outside the visible spectrum, when it is too expensive to produce the large detector arrays, this scheme gives us a better solution by using only one pixel. Combining this system with the "smashed filter" technique, we hope to create an efficient IR gas sensor. We performed Matlab simulations to evaluate the effectiveness of the smashed filter for gas tracing.
Keywords: compressive sensing, Echelle spectrometer, smashed filter, gas tracing

1. COMPRESSIVE SENSING

The dominant theory in the signal processing world is the well-known Shannon sampling theorem which claims that when sampling a signal (e.g., converting from an analog signal to digital) the sampling frequency must be greater than twice the bandwidth of the input signal in order to be able to reconstruct the original image/signal [1]. The major problem of this sampling scheme is: it neglects a fact that almost all the natural images/signals have certain structures embedded. CS goes against the conventional wisdom by suggesting that one can recover certain signals and images from far fewer measurements than those based on Shannon theory. Based on CS, we built the unique single-pixel camera system and it should be a good example to help one understand CS.

Rice Single-pixel Camera (SPC): What Makes It Possible?

Without any knowledge of CS, one could hardly imagine that an imaging system with only one detector element could, without scanning, produce a good quality high resolution image.

If you want a 1 megapixel (MP) image, what do you do? The most direct way is to take the picture using a digital camera which has a one million pixel array of photo-detectors working together to record images as a series of points called pixels. The light values are converted into a huge set of numbers and these numbers are then compressed using methods such as JPEG, JPEG2000, MPEG etc. For example, JPEG compression performs a discrete cosine transform on this set of numbers and more than 90% of the transformed coefficients, which are zeroes or close to zeroes, are thrown away. The inherent inefficiency problem with "acquire first and compress later" scheme leads us to the question, "Why do we take 100% of the measurement when we only need few of them to create an image?"

To get the same 1 MP resolution with a single element detector, one can employ a scanning scheme. This requires collection of 1 million serial measurements first and then assembling them to get the 1MP image, which is among other things, very time consuming.

Unlike the two schemes above, in our SPC system, an image of the scene is collected and projected by a lens onto a digital micromirror device (DMD) [2], fabricated by Texas Instruments. DMDs are primarily used in digital televisions and projector systems to digitally modulate light. Each DMD consists of millions of micromirrors whose orientation can be precisely controlled to tilt either 12 degree or -12 degree about its diagonal. This switching function is controlled by a computer and directly corresponds to the elements of a binary matrix. Light from the scene is then tuned as a white noise and split into two paths. Either of these two paths can be focused by a second lens onto a photodiode which converts the light signal to photovoltage. Each time the mirrors shift, a new photovoltage value will be generated by the photodiode and recorded along with the mirror configuration which produced it. The original image is then reconstructed from this series of photovoltage values, by using certain nonlinear optimization algorithms. The schematic of the SPC setup is displayed in Figure 1.

Unconventional Imaging, Wavefront Sensing, and Adaptive Coded Aperture Imaging and Non-Imaging Sensor Systems, edited by Jean J. Dolne, Thomas J. Karr, Victor L. Gamiz, Stanley Rogers, David P. Casasent, Proc. of SPIE Vol. 8165, 81650E · © 2011 SPIE · CCC code: 0277-786X/11/$18 · doi: 10.1117/12.894191

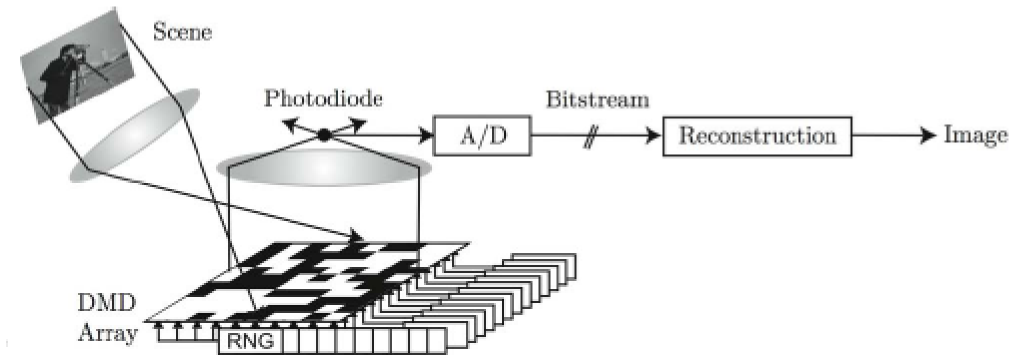

Figure 1. Single-pixel camera schematic

Actually, the overall design of this single pixel imaging system was inspired by the CS theory which states that it is possible to reconstruct images or signals of interests accurately from a number of samples far smaller than the desired resolution of the image/signal.

2. ECHELLE SPECTROSCOPY

CS is a very powerful theory which suggests that a small group of non-adaptive linear projections of a compressible signal or image contains enough information for reconstruction. The design of the single pixel camera exploits this idea by directly acquiring random projections of a scene without first collecting the pixels. One of the beauties of this architecture is its ability to get an image, or even a video, with a single detection element while sampling the scene many fewer times than the number of pixels. For some wavelengths outside the visible spectrum, when it is too expensive to produce the large detector arrays, this scheme gives us a better solution by using only one pixel. Now by inserting a dispersive element, such as a prism or grating, the camera system can function as a spectrometer. Since our light modulator DMD is 2-dimensional, we can design our dispersion to be that as well.

2.1 An Echelle Grating and Its Properties

The term *Echelle* denotes a special diffraction grating with rather coarse groove spacing (23-316 grooves/mm available from Newport Company) used at high angle of incidence (typically 32º, 44º, 63.5º, 71.5º, and 79º) with high diffraction orders (usually 10-100). Some important properties of Echelle gratings are listed below.

2.1.1 Need Cross Dispersion

Gratings are used to produce a double series of the repeated spectra through diffraction. The traditional spectrographs, which generally use one dispersive element, either a grating or prism, usually operate in 1st or 2nd order. However, an Echelle grating is specially designed to work in very high diffraction orders resulting in the overlapping between successive orders. Thus, a second dispersive element, either a prism or low dispersion grating is needed to disperse the light in the direction perpendicular to the Echelle grating to separate the overlapping orders. The resulting two-dimensional spectrum (called an Echellogram), which is a stack of the spectra from successive orders, can be ideally projected on a two-dimensional detector such as a CCD camera. Two sample Echllelograms taken by a CCD camera from our visible prototype are displayed in Figure 3. The spectra go from blue at the bottom left corner to red at the top right corner. The bright spots in the spectra correspond to different wavelengths from the neon and argon spectral calibration lamps, which clearly show that each line is a continuous progression of spectral information and not just a single wavelength spread in a second dimension.

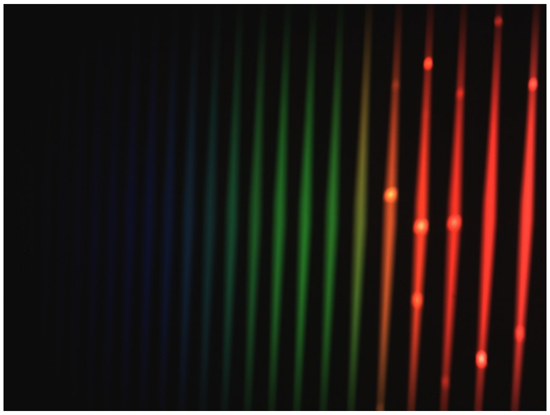

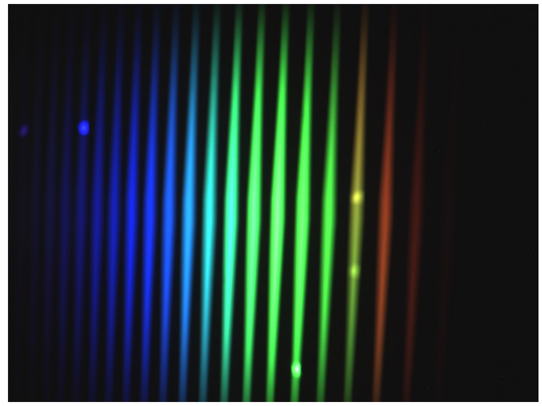

Figure 3. Spectrum from a white light source + neon calibration lamp (left); spectrum from the same white lamp + argon calibration lamp + CuSO4 as filter (right)

2.1.2 High Angular Dispersion and Resolving Power

Two views of the Echelle section (from Schroeder, D. J. 1970. Publ. Sstron. Soc. Pac. 82: 1253-1275) are shown in Figure 4, where α, β, and θ_B are the incidence, refraction and blaze angles in the YZ plane, γ is the angle between the incident light and the YZ plane, and σ is the groove spacing of the Echelle. Equations of the angular dispersion and resolving power for a general grating working in the littrow mode are listed as followings

$$d\beta / d\lambda = (2/\lambda)\tan\theta_B \quad (1)$$

$$R = (2W\sin\theta_B)/\lambda = 2D\tan\theta_B/\lambda \quad (2)$$

where W denotes the ruled width of the grating and D is the beam diameter prior to entering the Echelle grating.

For a normal first order grating, typically $\tan\theta_B = 1/2$, while for an Echelle grating with the blaze angle of 63.5º, $\tan\theta_B = 2$. Thus, an Echelle gives higher angular dispersion and resolving power than the traditional low blaze-angle grating.

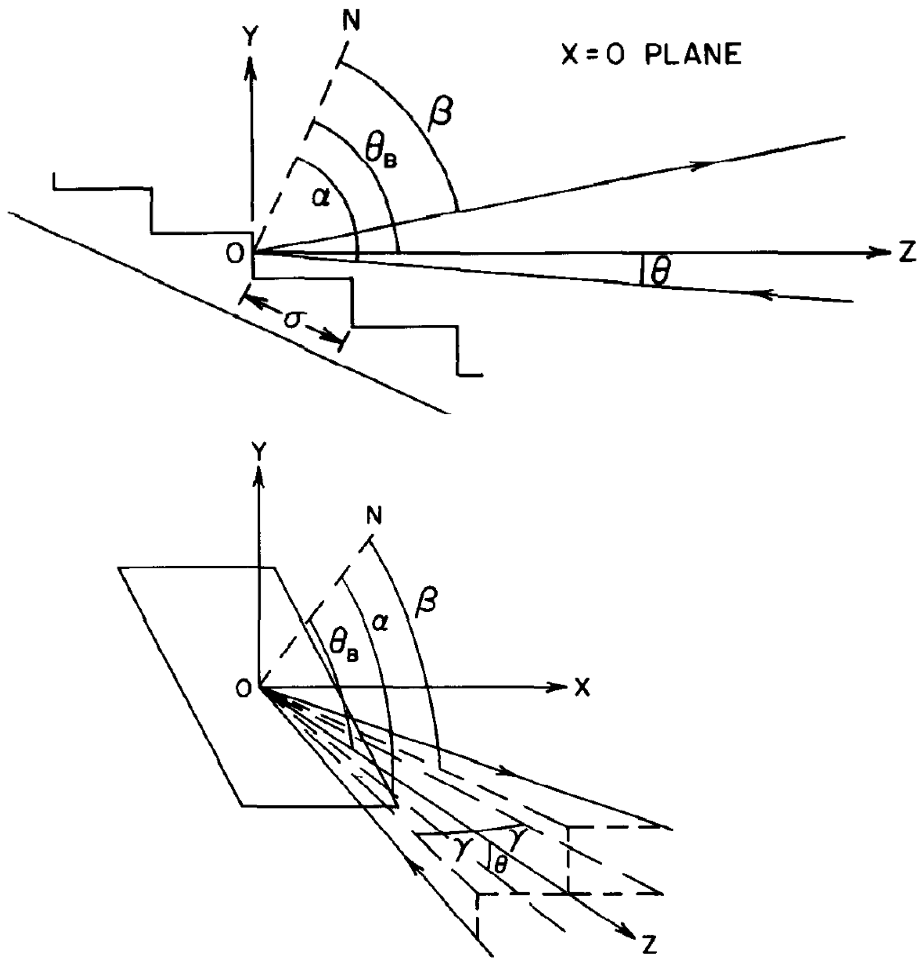

Figure 4. Two views of the Echelle section

2.2 Experiment Setup

2.2.1 The Configuration of the Traditional Echelle Spectrometer

Figure 5 shows a sketch of the conventional Echelle spectrometer setup (from the technical note of the Newport Company). The light from a slit or pinhole is collimated, usually by a concave mirror as shown, and then hits the Echelle grating. The Echelle grating is tilted at the blaze angle for the Littrow mode. Another cross disperser, a prism in the picture, is used to separate the overlapping orders from the Echelle. The resulting two-dimensional spectrum is focused by a camera mirror onto the CCD detector.

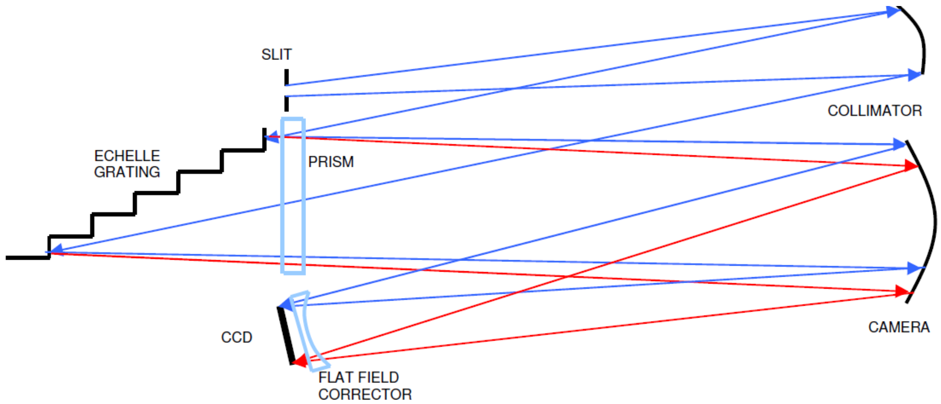

Figure 5. Sketch of a conventional Echelle spectrometer setup

2.2.2 Compressive Echelle Spectrometer Setup

In our compressive spectrometer system, the CCD camera is replaced with the light modulator DMD on which series of random patterns are projected. Light reflected from the DMD is focused by a lens onto the single detector.

Figure 6 displays the drawing of our compressive system and Table 1 lists the specification of all the elements used in our visible setup.

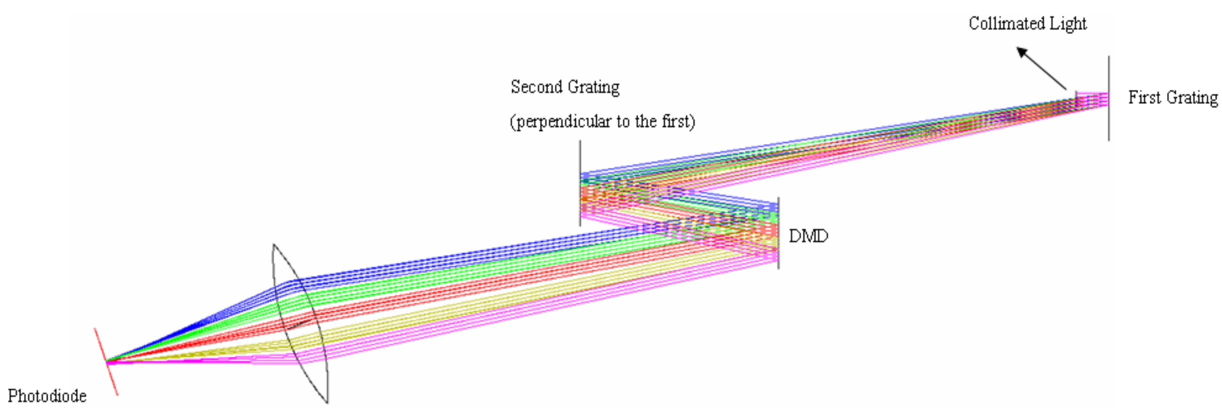

Figure 6. Sketch of our compressive Echelle spectrometer setup

Table 2. Specifications of the elements used in the visible prototype

Light Source	Schott DCR III fiber optic illuminator 150 Watt halogen lamp
Pinhole	300μm aperture diameter
Collimator	Ø2" silver-coated concave mirror, f=150 mm
Echelle Grating	25mm x 50mm, 54.5 grooves/mm, 46º blaze angle, working in Littrow mode
Cross Disperser	Visible transmission grating, 300 grooves/mm, 17.5° blaze angle, 25 x 25 mm
First Focusing Element	Ø2" achromatic doublet, f=100 mm, ARC: 400-700nm
DMD	D1100 with 96 Gigabits memory on board
Second Focusing Element	27.5mm EFL focusing instrument eyepiece
Detector	A photomultiplier (PMT) module, model number H9306-03, from Hamamatsu Company, wavelength range185-900nm, peak wavelength 450nm, rise time 1.4ns, effective area 13mm

2.3 CS Data

The *TVAL3* solver [7] is used as the reconstruction tool for results shown in Figure 7.

As is evident from Figure 7, the ratio of measurements to resolution required for the reconstruction of the same or even better quality of image drops with the increase of the resolution. This phenomenon could be attributed to the fact that the sparsity of the image does not increase as fast as the resolution increases, and thus relatively fewer percent of measurements are needed in the reconstruction step. To better show how the wavelengths spread along different lines/orders, several cutoff filters are inserted just after the light source. The resulting spectra at a resolution of 256 x 256 and 20% measurements are shown in Figure 8. These data can also be used for future wavelength calibration analysis.

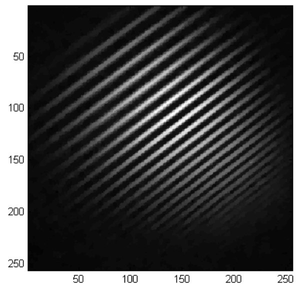

256 X 256 (30% coeffs)

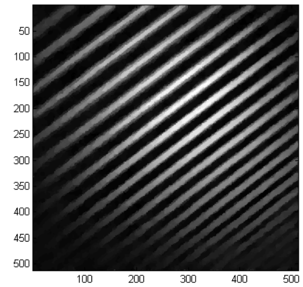

512 X 512 (10% coeffs)

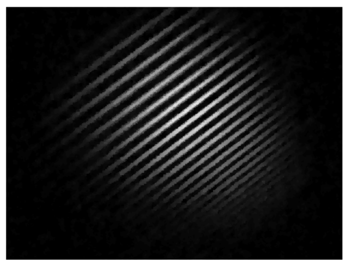

1024 X 768 (5% coeffs)

Figure 7. Reconstructed spectra at different resolutions with different percentage of measurements

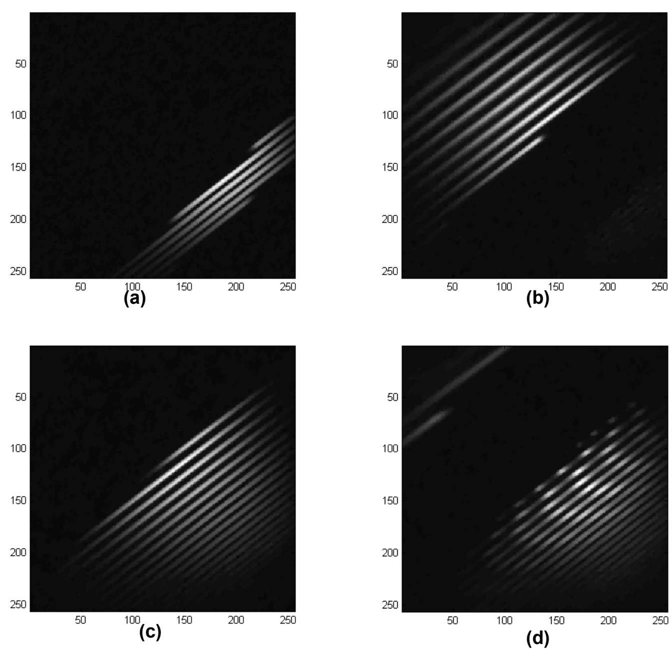

Figure 8. Reconstructed spectra with (a) 500 – 550nm band pass filter (b) 633nm long pass filter (c) 650 short pass filter (d) 785nm Raman long pass filter

2.4 Future Application

As we have demonstrated the proof-of-concept of our visible prototype, we will discuss how we apply this in the IR spectroscopy. As mentioned above, compared with its counterpart, our system will greatly reduce the cost when doing the spectroscopic applications beyond visible. Figure 9 shows the absorption spectra of several types of gas. A quick inspection reveals that some of them are overlapping. We hope to create an efficient IR gas sensor by combing our compressive system with an effective mathematical method. Now we will outline how we will use this to detect target gases with far fewer measurements as compared to the case of imaging.

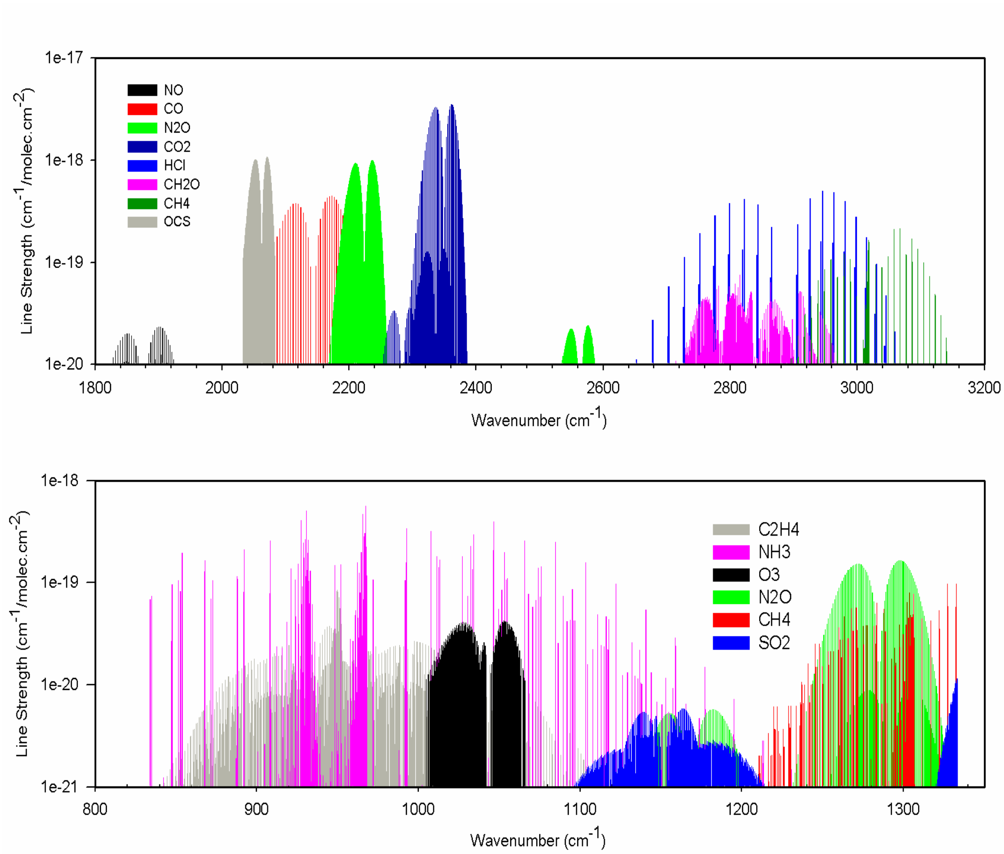

Figure 9. Sample absorption spectra of several types of gas from HITRAN database

2.4.1 Smashed Filter for Target Classification

CS enables us to recover an image from a set of random projections by exploiting its sparsity in some basis. However, in most applications, we are not interested in reconstructing a complete, precise image of an object, but rather want to detect the presence of that object of it. Target detection or classification is an example. Davenport, et al, combined the generalized maximum likelihood hypothesis (matched filter) with compressed sensing and worked out a new technique dubbed the "smashed filter" [8]. The smashed filter concept is that, for classification and detection purposes, we can directly analyze the compressive measurements, which are very small in number when compared to the reconstruction of the overall image.

2.4.2 Simulation Results

We performed a simulation in Matlab to evaluate the effectiveness of the smashed filter for gas classification in IR. We collected a library [9] for 14 different gases with the absorption spectra in the range of 1 ~ 2.8 microns (corresponding to the wave number from 3571.4 ~ 10000 cm^{-1}). The gases include C_2H_2, CH_4, CO, CO_2, H_2O, HBr, HCl, HF, HI, N_2O, NO, O_2, O_3, and OH which are numbered from 1 to 14 respectively. Their absorption spectra can be seen in Figure 10.

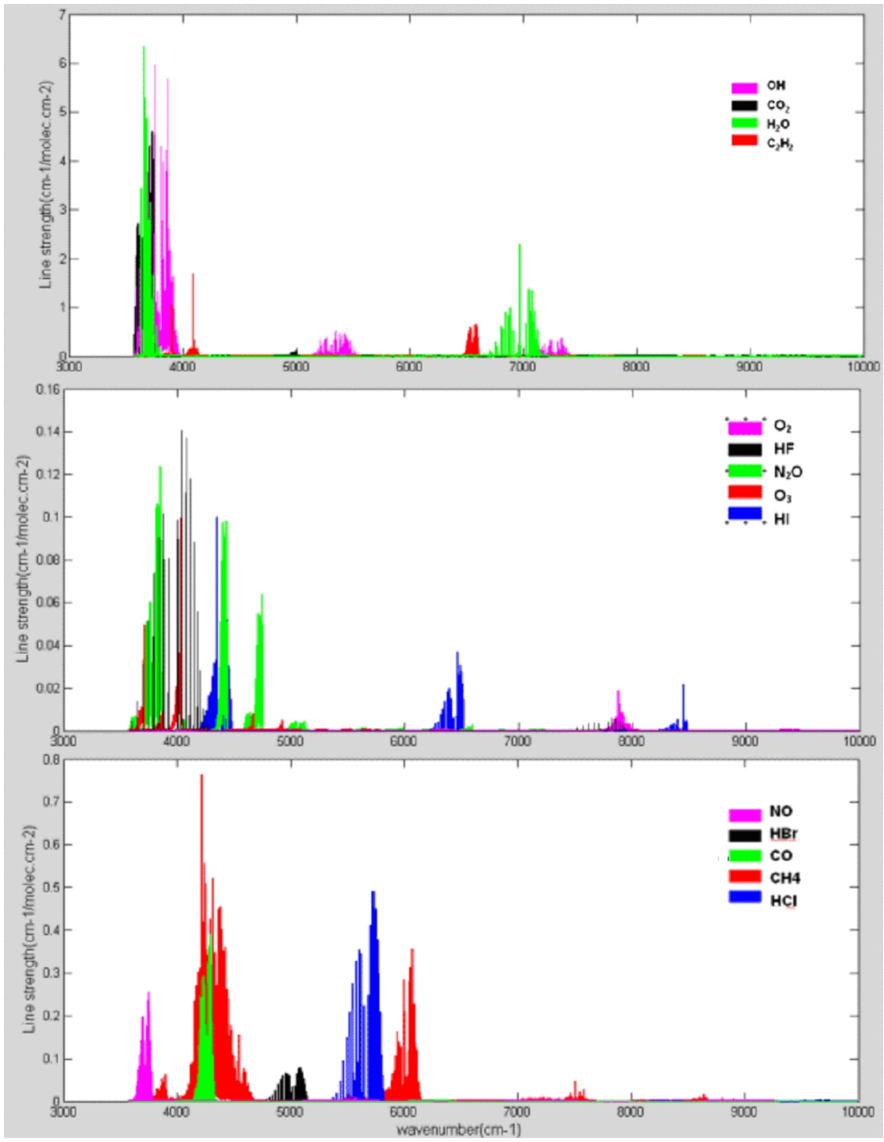

Figure 10. Plots of the absorption spectra of 14 different gases

First, we chose 4 gases C_2H_2, CO, CO_2 and O_3 to generate a composite test gas with the percentage of 15, 20, 60 and 5 respectively. Their individual spectra and the total spectrum are shown in Figure 11. Followings are some preliminary results from the simulation.

In noiseless case, as evident in Figure 12, for an spectrometer system with the resolution of 6500 pixels, which is close to our current prototype system, as few as 30 percent of measurements (about 0.46%) can give us a perfect detection with the mean square error equal to 0.006. Somewhere we only see the red circle, that's because the red (recovered coefficients) are overlapping with the blue (original coefficients). However, in real world, we can not avoid noise, so we add noise in the test spectrum which is shown in Figure 13 with certain spectral part enlarged. In this case, for a spectrometer system with 256 pixels which is the typical resolution for a commercial IR spectrometer, even with 100% measurements, it fails to tell the 4 gases apart. When we increased the resolution back to 6500, the same number of 256 measurements (3.93%) can roughly detect the 4 gases. Increasing the measurements to 400, which corresponds to 6.15% of the total resolution, we can almost precisely tell them apart. The corresponding results are displayed in Figure 14, 15, and 16 respectively. The simulation shows the effectiveness of the smashed fitler method for target detection in the compressive sensing field. We also notice here that the success of this method also depends on the system resolution. That's why we are working on the compressive Echelle system which can give higher resolution but with the reduced cost.

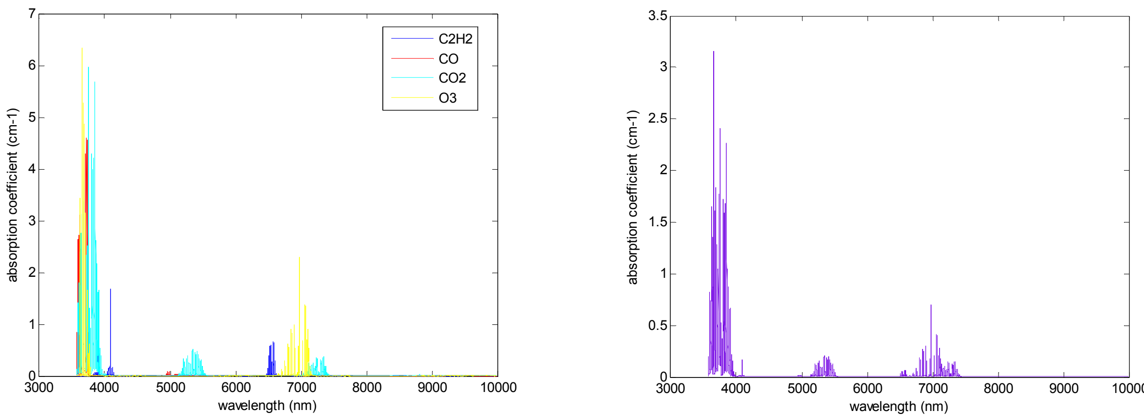

Figure 11. Individual spectra and the created composite spectrum of 4 gases

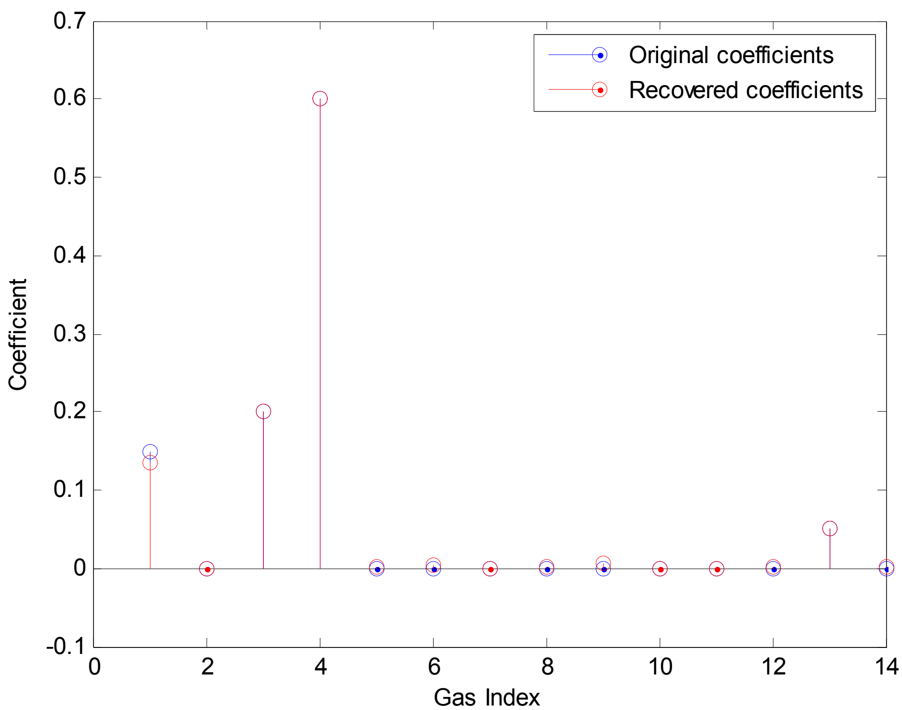

Figure 12. Noiseless, 6500 pixesl, recovered coefficients vs. original coefficients with 0.46% (30) measurements ($\sigma = 0.006$)

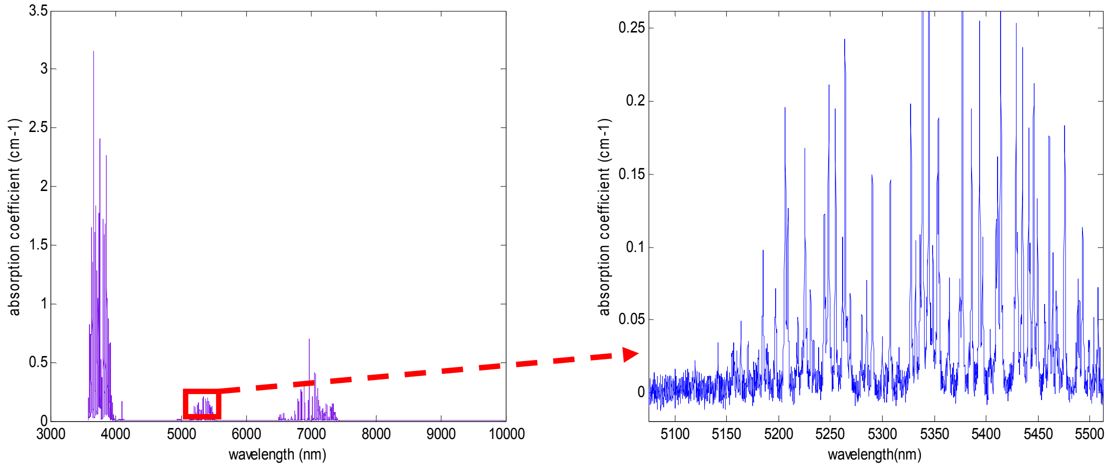

Figure 13. Test spectrum with the added noise

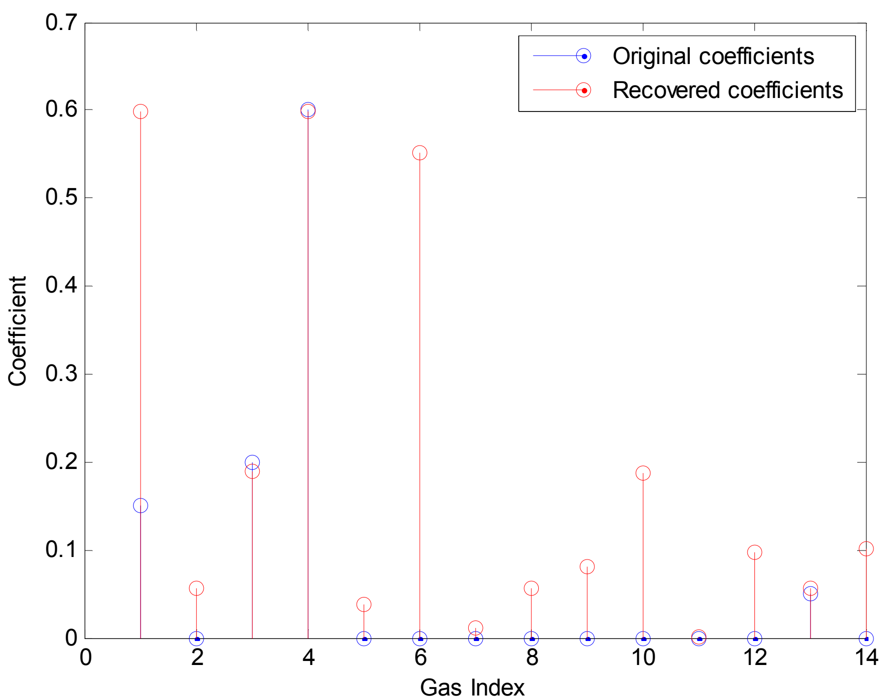

Figure 14. Noisy case, 256 pixels, recovered coefficients vs. original coefficients with 100% (256) measurements ($\sigma = 0.758$)

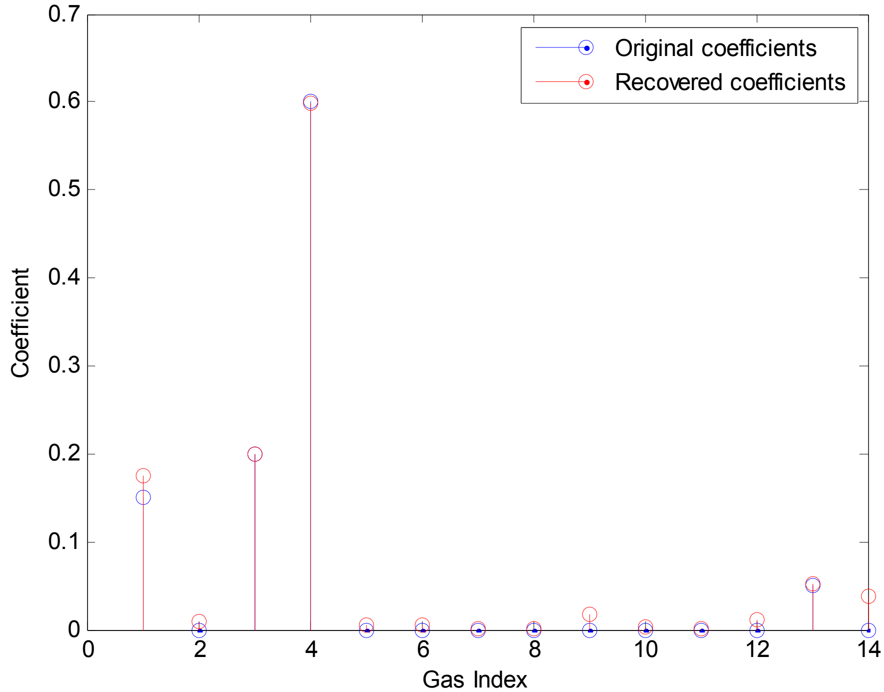

Figure 15. Noisy case, 6500 pixels, recovered coefficients vs. original coefficients with 3.93% (256) measurements ($\sigma = 0.055$)

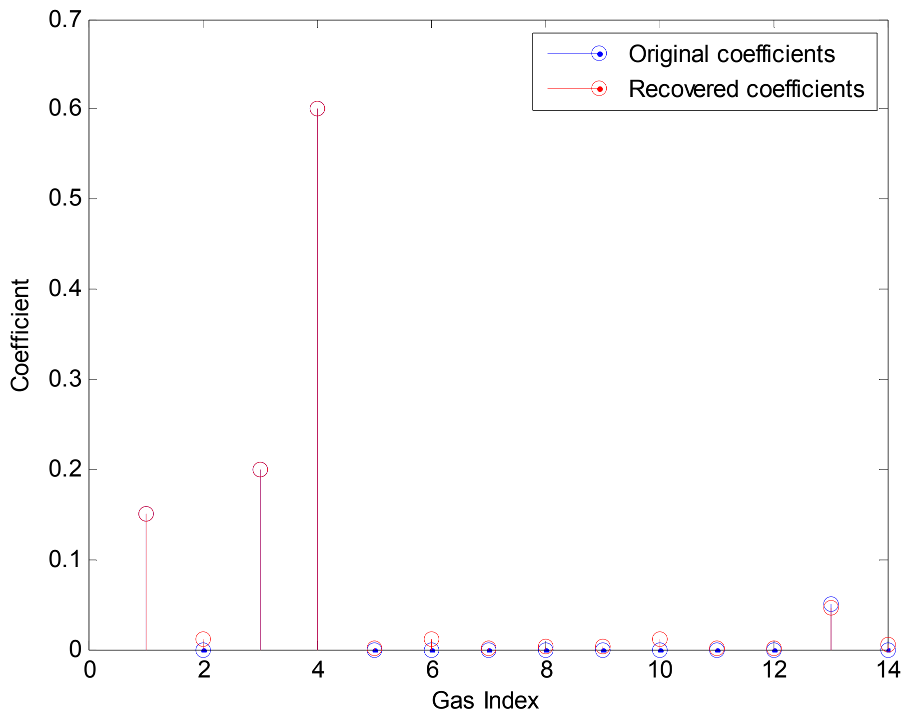

Figure 16. Noisy case, 6500 pixels, recovered coefficients vs. original coefficients with 6.15% (400) measurements ($\sigma = 0.022$)

REFERENCES

[1] C. E. Shannon, “Communication in the presence of noise," Proceedings of the IEEE, vol. 86, NO. 2, (1998)

[2] J. Sampsell, “An overview of the digital micromirror device (DMD) and its application to projection display,” SID Int. Symp. Digest of Technical Papers, vol. 24, p. 1012, (1993)

[3] D. J. Schroeder, "Echelle Efficiencies: Theory and Experiment; Author’s Reply to Comment," Appl. Opt. vol. 20, NO. 4, p. 530-531, (1981)

[4] F. H. Chaffee, Jr, D. J. Schroeder, “Astronomical Applications of Echelle Spectroscopy,” Annual Review of Astronomy and Astrophysics, vol. 14, p. 23-42, (1976)

[5] D. J. Schroeder, “ Design Considerations for Astronomical Echelle Spectrographs,” Publications of the Astronomical Society of the Pacific, Vol. 82, No. 490, p.1253, (1970)

[6] D. J. Schroeder, C. M. Anderson, “Echelle Spectrograph for Astronomical Use,” Pub. Astron. Soc. Pacific, vol. 83, (1971)

[7] C. Li, W. Yin, Y. Zhang, “TVAL3: TV minimization by Augmented Lagrangian and ALternating direction ALgorithms **,”** available at http://www.caam.rice.edu/~optimization/L1/TVAL3/

[8] M. A. Davenport, M. F. Duarte, M. B. Wakin, J. N. Laskar, D. Takhar, K. F. Kelly, R. G. Baraniuk, “The Smashed Filter for Compressive Classification and Target Recognition,” Proc. of Computational Imaging V at SPIE Electronic Imaging, (2007)

[9] http://spectra.iao.ru/1440x725/en/home/